Monatshefte für Chemie 126, 519–527 (1995)

Monatshefte für Chemie
Chemical Monthly

Cyclic Voltammograms of Iron and C-Steels in Oxalic Acid Solutions and Investigation of the Effect of Phenyl Phthalimide as Corrosion Inhibitors

M. Abdallah and **H. E. Megahed**

Chemistry Department, Faculty of Science, Benha University, Benha, Egypt

Summary. The electrochemical behaviour of Fe and C-steel samples in oxalic acid solutions was studied by the use of cyclic voltammetry. Two peaks were observed; the first one was the anodic peak and the second one an unexpected reductive dissolution peak which could be observed in the cathodic branch of cyclic voltammograms of all electrodes studied. The carbon content was found to increase the active dissolution of steels and to decrease their tendency towards passivation. The inhibitive efficiency of phenyl phthalimide derivatives on the active dissolution of Fe and steel samples in 0.1 *M* oxalic acid were investigated.

Keywords. Oxalic acid; Phenyl phthalimide; C-steel; Cyclic voltammetry; Corrosion inhibitors.

Cyclische Voltammogramme von Eisen und C-Stählen in Oxalsäurelösungen und der Einfluß von Phenylphthalimiden als Korrosionsinhibitoren

Zusammenfassung. Das elektrochemische Verhalten von Eisen und C-Stählen in Oxalsäurelösungen wurde mit Hilfe cyclischer Voltammetrie studiert. Dabei treten zwei Signale auf: das anodische Signal sowie ein unerwartetes reduktives Lösungssignal. Letzteres wurde im kathodischen Zweig der cyclischen Voltammogramme aller untersuchten Elektroden gefunden. Der Kohlenstoffgehalt erhöht die aktive Auflösung von Stählen und erniedrigt ihre Tendenz zur Passivierung. Die Inhibitionseffizienz von Phenylphthalimiden für die aktive Auflösung von Eisen und Stahlproben in 0.1 *M* Oxalsäure wurde untersucht.

Introduction

In various industrial, processes oxalic acid comes in contact with metallic apparatus. It is extensively used as neutralizer after cleaning and leaching in the fiber industry and as a pickling agent in metallurgy. In previous papers, some investigations on metallic corrosion in oxalic acid were carried out by measuring the weight loss and polarization curves under the same conditions [1–4].

Inhibition efficiency of organic compounds is strongly dependent on the structure and chemical properties of the layer formed on the metal surface under particular experimental conditions. In the case of nitrogenous compounds in acidic

media, the adsorption process is ascribed to effects connected with aromatic rings. It has been reported that the adsorption of nitrogenous compounds occurs with aromatic rings parrallel to the metal surface [5]. It has been observed that the adsorption appears to depend mainly on the electronic structure of the molecule and that the inhibition efficiency increases with the length of the hydrocarbon chain of the organic compound and the number of aromatic rings [6–8].

In the present work, cyclic voltammograms of iron and C-steel electrodes were studied in oxalic acid solutions. The effect of acid concentration on these cyclic voltammograms was also investigated. The effect of four derivatives of phenyl phthalimide as corrosion inhibitors on the anodic branch of the cyclic voltammograms of iron and C-steel electrodes was examined in 0.1 *M* oxalic acid.

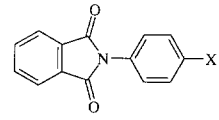

1: X = H; **2**: X = CH_3; **3**: X = COOH; **4**: X = Cl

Results and Discussion

Cyclic Voltammograms of Fe and C-Steel Electrodes in 0.1 M Oxalic Acid

The curves in Fig. 1 represent the cyclic voltammograms (CVs) of Fe, steel I and steel II, respectively, in a 0.1 *M* oxalic acid solution. The starting potential was −2.0 V (*vs.* SCE) and the scanning range extended up to +2.0 V at a voltage scanning rate of 50 mV·sec^{-1}.

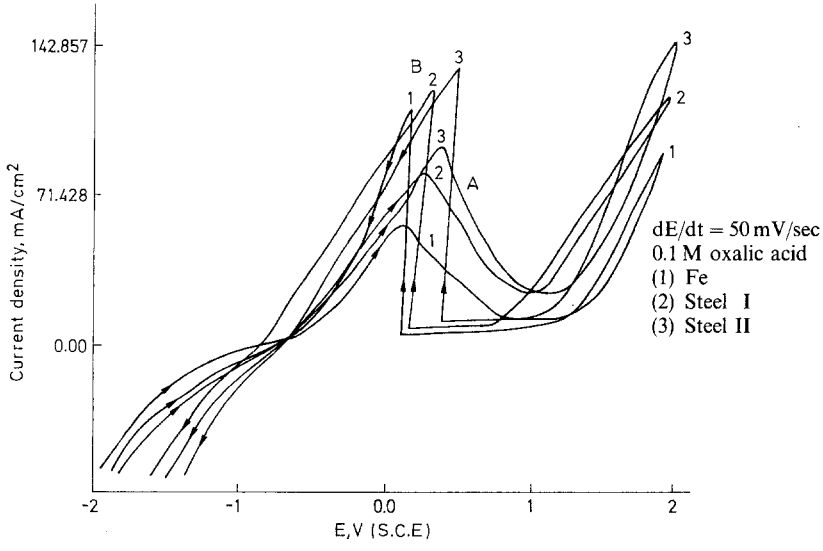

Fig. 1. Cyclic voltammograms of Fe, steel I and steel II in 0.1 *M* oxalic acid at a sweep rate 50 mV·sec^{-1}

From an inspection of the curves in Fig. 1, the following features can be recognized:

(*i*) As the potential of the electrode is shifted into the noble direction, an increase in the anodic current density is noted, representing the active dissolution of Fe as Fe^{2+} (peak A). This is fairly well represented by a *Tafel* type relationship [9].

(*ii*) A region of slow decrease of current covering a certain potential range. This region is characteristic of an active-passive transition [10].

(*iii*) At a certain definite potential, the current drops to low values indicating the onset of passivity. The electrode is considered now to be covered by a pore-free passivating oxide film of mainly trivalent iron (γ-Fe_2O_3). These potentials are commonly identified as the *Flade* potentials [11]. γ-Fe_2O_3 can be formed in the film covering the electrode surface by the oxidation of Fe^{2+} ions according to [12]:

$$2\,Fe^{2+} + 3\,H_2O \rightarrow \gamma\text{-}Fe_2O_3 + 6\,H^+ + 2\,e^- \qquad 1$$

(*iiii*) As the potential becomes more positive, the current rises again to form the transpassive region before oxygen evolution commences.

Further inspection of the curves in Fig. 1 reveals that, the current drops to a zero value along the passive region when the potential of the electrode is reversed into the cathodic direction after oxygen evolution. At a certain potential (nearly the passivating potential), another dissolution peak (peak B) is obtained instead of any expected cathodic reduction peaks. The amount of reductively dissolved Fe during cathodic reduction of the anodic oxide film formed on Fe in boric-borate solutions was found to exceed the amount calculated from the charge of the anodic oxide film, assuming Fe(III) is formed [13]. This phenomenon was attributed to the dissolution of underlying Fe which would occure at a higher rate in acid solution.

Sato, *Kuda*, and *Noda* proposed a model of an anodic oxide film formed on Fe in boric- borate solutions in which the inner layer consists of anhydrous Fe_2O_3, probably containing excess oxygen ions depending on the potential (increases with increasing potential), and the outer layer is hydrous Fe_2O_3 containing bound H_2O [13]. The boundary between the layers is not distinct, and the layers are diffusing into each other during the anodic polarization. The bound H_2O serves as a donor of electrons and protons. Protons will diffuse out of the oxide leaving excess oxygen ions. At high positive potential, most of the space change will be excess oxygen ions because of the depletion of electrons. Based on this model of the anodic oxide film on Fe, it is reasonable to assume that in the cathodic direction (especially at the peak potential of peak B) there are two possible cathodic reactions. The first one is the formation of H_2O by diffusion of protons in the oxide film forming H_2O. This reaction consumes cathodic charges which are imposed to the electrode. The second is the reductive dissolution of the oxide film. The cathodic charges required for this reaction are available from the dissolution of the metallic Fe according to the following mechanism [14]:

$$\text{Anode: } Fe \rightarrow Fe^{2+} + 2\,e^- \qquad 2$$

$$\text{Cathode: } 2\,Fe^{3+} + 2\,e^- \rightarrow 2\,Fe^{2+} + \quad (\text{anion vacancy}) \rightarrow 2\,Fe^{2+}\,(aq) \qquad 3$$

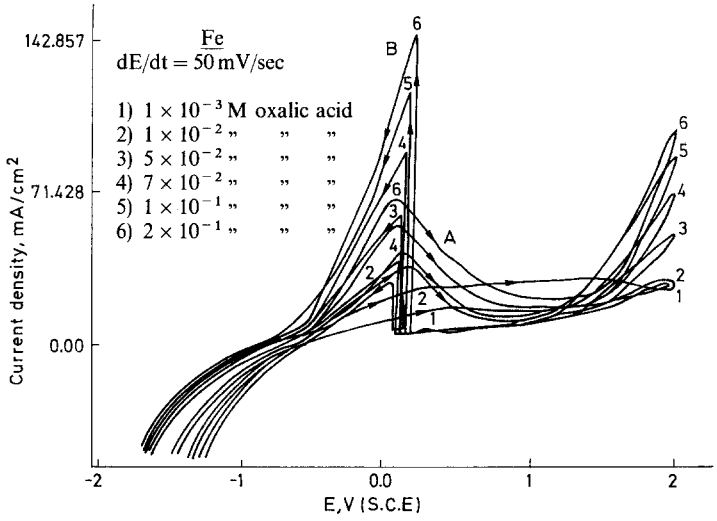

Fig. 2. Cyclic voltammograms of Fe in varying concentrations of oxalic acid at a sweep rate $50\,mV \cdot sec^{-1}$

These reactions are only possible in oxides containing cations of variable valency [14]. It is to be assumed that these reactions may occur since it was observed that the iron ions in the passivating oxide film are mainly Fe (III) with only small amounts of Fe (II) [13]. Furthermore, in the cathodic direction and at the peak potential of peak 'B', the presence of cracks in the oxide film may create a local cell between the bare metal and the remaining oxide film, thus leading to the occurrence of localized types of corrosion as demonstrated by *Cohen* and *Oswin* [15] for the anodic oxide film formed on Fe in borate buffer solutions.

Effect of Acid Concentrations on the Cyclic Voltammograms of Iron and C-Steels

Fig. 2 shows the cyclic voltammograms of the Fe electrode in varying concentrations of oxalic acid at a scanning rate of $50\,mV \cdot sec^{-1}$ as an example. Steel I and steel II show the same shape of cyclic voltammograms (not shown). Table 1 shows the effect of the acid concentrations on peak potential (E_p), peak current density (i_p) of peak A, *Flade* potential (E_F), and peak current density (i_p) of peak B. The values in Table 1 show that an increase of the acid concentration leads to:

(i) an increase of peak current (i_P) and a shift of the peak potential (E_p) for peak A for all electrodes toward less positive values
(ii) an increase of i_p for peak B for all electrodes
(iii) a shift of the *Flade* potential (E_F) of all samples toward more positive values

Effect of the Carbon Content on the Dissolution of Steel Samples in Oxalic Acid

Inspection of Table 1 and Fig. 1 reveals that at any acid concentration, the increase of the C-content of steel samples increases the current density of the dissolution peak 'A'. This indicates that corrosion of steel increases with increasing C-content of the sample. The peak potential of peak A and the *Flade* potential are shifted to

Table 1. Effect of acid concentration on peak potential (E_p), *Flade* potential (E_F), and peak current density (i_p) for anodic (A) and cathodic (B) peaks

Acid conc.	E_p (mV *vs.* SCE)			E_F (mV *vs.* SCE)			i_p (mA/cm^2) for peak A			i_p (mA/cm^2) for peak B		
	Fe	steel I	steel II	Fe	steel I	steel II	Fe	steel I	steel II	Fe	steel I	steel II
$1 \times 10^{-3}\,M$	–	–	–	–	–	–	22.857	–	–	29.924	33.068	37.142
$1 \times 10^{-2}\,M$	–	250	–	–	550	730	31.428	42.857	45.714	41.323	56.998	42.856
$5 \times 10^{-2}\,M$	170	200	420	580	605	825	37.143	56.785	58.571	64.123	66.548	72.856
$7 \times 10^{-2}\,M$	110	141	360	620	685	910	44.643	64.286	67.143	92.622	95.472	102.142
$1 \times 10^{-1}\,M$	80	100	223	710	790	990	62.857	75.714	87.143	115.423	121.12	129.998
$2 \times 10^{-1}\,M$	20	82	201	790	932	971	70.000	84.286	97.143	142.857	148.195	156.748

more positive values with increasing the C-content, indicating a decreasing tendency toward passivation.

The increase of the corrosion rate with increasing C-content of steel can be explained on the basis of a cathodic controlled mechanism. Thus, upon increasing the C-content, the pearlite phase is increased on the expense of the ferrite phase [16]. Since the hydrogen overvoltage on pearlite is lower than on ferrite [17], the increase of the former increases the cathodic areas of lower hydrogen overvoltage and consequently the corrosion rate.

Effect of Addition of Phenyl Phthalimide Derivatives on the Dissolution of Fe and C-Steel Electrodes in 0.1 M Oxalic Acid

The effect of addition of increasing concentrations of some phenyl phthalimide derivatives on the anodic branch of the CVs of Fe, steel I, and steel II electrodes in 0.1 *M* oxalic acid at a sweep rate $50\,mV \cdot sec^{-1}$ were studied. Figure 3 represents the effect of compound **4** on the anodic branch of the CVs of a steel II electrode. Similar curves were obtained using other compounds for Fe and C-steel samples (not shown). Table 2 shows the data obtained from these curves.

The inhibition efficiency was calculated from equation 4:

$$I.E. = 100 \cdot \left(1 - \frac{i_{p(add)}}{i_{p(free)}}\right) \qquad 4$$

where $i_{p(add)}$ and $i_{p(free)}$ are the peak current densities in presence and absence of inhibitors.

Inspection of the curves of Fig. 3 and Table 2 indicates that an increasing concentration of these compounds shifts E_p to more positive values and i_p to lower values, thus increasing the inhibition efficiency. This indicates an increased resistance to active dissolution which depends on both the type of electrode and the inhibitor.

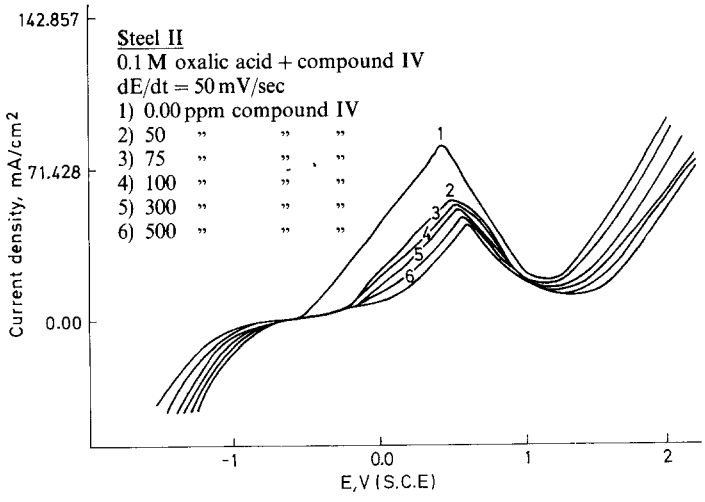

Fig. 3. Effect of concentration of compound **4** on the anodic branch of the cyclic voltammogram of steel II at a sweep rate $50\,mV \cdot sec^{-1}$

Table 2. Effect of inhibitor concentrations on the peak current density (i_p) and inhibition efficiency (*I.E.*) for dissolution of Fe and C-steel samples in 0.1 *M* oxalic acid

Inhibitor concentration	i_p (mA/cm^2)			*I.E.*		
	Fe	steel I	steel II	Fe	steel I	steel II
0.1 *M* oxalic acid + compound **1**						
0.00 ppm compound **1**	61.404	72.828	84.252	–	–	–
50 " " "	42.840	51.408	55.714	30.23	28.91	33.87
75 " " "	37.128	46.410	51.728	39.53	35.82	38.60
100 " " "	35.700	42.840	45.000	41.86	40.76	46.58
300 " " "	31.416	39.984	38.232	48.84	44.71	54.62
500 " " "	28.560	32.130	31.428	53.49	55.57	62.69
0.1 *M* oxalic acid + compound **2**						
0.00 ppm compound **2**	61.404	72.828	84.252	–	–	–
50 " " "	39.270	35.550	51.408	36.05	25.95	38.98
75 " " "	31.416	49.980	44.982	48.84	30.88	46.61
100 " " "	25.704	44.268	35.700	58.14	38.78	57.63
300 " " "	22.848	40.698	29.988	62.79	43.72	64.41
500 " " "	17.850	34.272	24.276	70.93	52.61	71.18
0.1 *M* oxalic acid + compound **3**						
0.00 ppm compound **3**	61.404	72.828	84.252	–	–	–
50 " " "	52.836	62.832	58.548	13.95	13.72	30.51
75 " " "	49.980	56.406	55.692	18.60	22.55	33.89
100 " " "	44.268	48.980	49.980	27.91	32.74	40.68
300 " " "	41.412	42.840	39.984	32.56	41.17	52.54
500 " " "	35.700	35.700	35.700	41.86	50.98	57.63
0.1 *M* oxalic acid + compound **4**						
0.00 ppm compound **4**	61.404	72.828	84.252	–	–	–
50 " " "	57.143	63.546	59.563	6.94	12.74	29.30
75 " " "	52.836	60.690	55.714	13.95	16.67	33.87
100 " " "	44.268	58.548	51.398	27.91	19.61	38.99
300 " " "	42.840	57.120	43.132	30.23	21.57	48.80
500 " " "	39.984	53.550	38.232	34.88	26.47	54.62

At all inhibitor concentrations the inhibiting efficiencies of compounds **1**–**4** for different electrode samples increase in the following order:

$$\text{Fe: } \mathbf{2} > \mathbf{1} > \mathbf{3} > \mathbf{4}$$

$$\text{steel I: } \mathbf{1} > \mathbf{2} > \mathbf{3} > \mathbf{4}$$

$$\text{steel II: } \mathbf{2} > \mathbf{1} > \mathbf{3} > \mathbf{4}$$

This sequence can be explained on the basis that the CH_3 group in compound **2** has a positive inductive effect resulting in a higher localization of electrons at the nitrogen atom, whereas the COOH group and the Cl atom in compounds **3** and **4** have a positive mesomeric effect which tends to increase the delocalization of electrons on the nitrogen atom.

The inhibiting effect of these compounds on the corrosion of iron and C-steel in oxalic acid increases with increasing electronegativity of the substituent. Introduction of nucleophilic (electron donor) substituents leads to an increase of adsorbability because of the increase of the π-electron density in the aromatic nucleus. Introduction of electron acceptor substituents has the opposite effect [18].

The inhibiting effect of these compounds may be attributed to their adsorption of such compounds at the metal solution interface. The chemisorption process takes place by the formation of a chemical bond between the metal and the adsorbed molecule, which depends on the nature of the metal and the molecular structure of the inhibitor. Chemisorption involves charge sharing or charge transfer from the inhibitor molecule to the metal surface to form a coordinate-type bond. In fact, electron transfer is typical for transition metals having a vacant low energy electron orbital [19]. Concerning inhibitors, electron transfer can be expected with compounds having relatively loosely bound electrons [20].

Conclusions

1) Cyclic voltammograms were recorded for Fe and carbon steels in 0.1 *M* oxalic acid solutions. All curves were characterized by an anodic dissolution peak (peak A) due to active dissolution of Fe as Fe^{2+} ion. Furthermore, an unexpected reductive dissolution peak (peak B) was observed. It is due to the formation of H_2O in the oxide film by diffusion of protons into the oxide film from the solution, thus forming H_2O and reductive dissolution of the oxide film.
2) Increase of acid concentration leads to an increase of i_p, a negative shift of E_p for peak A, and an increase of i_p for peak B for all electrodes.
3) The increase of the C-content decrease the tendency of steel towards passivation.
4) Phenyl phthalimide derivatives can be used as corrosion inhibitors for the dissolution of Fe and C-steel in 0.1 *M* oxalic acid. The inhibition efficiency (*I.E.*) of these compounds was calculated from the value of *I.E.* was found to increase with increasing inhibitor concentrations and the electronegativity of the substituents.

Experimental

The chemical composition of pure iron and two C-steel electrodes used in this investigation are presented in Table 3. These samples were provided by the *Egyption Delta Steel Company Cairo.* The electrodes are fixed to pyrex glass tubings by neutral wax (exposed surface area for the electrodes: 0.14 cm^2) and the electrical contact is made through thick copper wires soldered to the end of the electrodes. The electrodes are successively abraded with finest grade emery paper and degreased with

Table 3. Chemical composition of the test electrodes

	%C	%Si	%Mn	%S	%P
Fe (pure)	–	–	–	–	–
Steel I	0.26	0.17	0.76	0.03	0.03
Steel II	0.40	0.16	0.66	0.025	0.035

acetone. Complete wetting of the surface was taken as indication of its cleanliness when rinsed with bidistilled water.

All chemicals used were of A.R. quality. The solutions were prepared using bidistilled water; no attempts were made to deaerate them. The electrolytic cell was all pyrex and is described elesewhere [21].

Cyclic voltammogram curves (CVs) were performed at a voltage scanning rate of $50\,mV \cdot sec^{-1}$ using Wenking Potentioscan Type POS-73. The current density-potential curves were recorded on a X-Y recorded type PL-3. All experiments were carried out at $25 \pm 1\,^{\circ}C$.

References

[1] Krapivkina T. A., Marchenko T. G., Martynovai I. N. (1985) Zasch Metal **21**: 258
[2] Shapovalov E. T., Kazakova G. V. (1983) Zasch Metal **20**: 929
[3] Ivascann S., Georgescu O (1979) Rev. Chim. **30**: 360
[4] Ivascann S., Georgescu O (1979) Rev. Chim. **30**: 568
[5] Schmitt G., Bedbur K. (1984) Proc 9th Int. Congr. on "Metallic Corrosion." Toronto, Canda, p 112
[6] Granese S. L. (1987) Proc 10th Int. Congr. "Metallic corrosion" Madras, India, p 2733
[7] Granese S. L. (1988) Corrosion **44**: 332
[8] Granese S. L., Degonzalez C. O., Rosales B. (1988) Quimindustria La Habana, Cuba **88**: 176
[9] Lorenz W. J., Ltibert F., Miyeshi Y., Eichkorn C. (1972) Proc. 5th. Int. Cong. Metallic Corros. (Toryo), p 74
[10] Abd El-Wahab F. M., Shams El-Din A. M. (1978) Br. Corrosion J. **13**: 39
[11] Vetter K. V. (1961) Elektrochem. Kinetik. Springer, Berlin
[12] Markoric T. (1964) Werkst. Korros. **15**: 543
[13] Sato N., Kuda K., Noda T (1971) Electrochem. Acta. **16**: 1909
[14] Scully J. S. (1975) The Fundamental of Corrosion, 2nd edn. Pergamon Press, p 118
[15] Cohen M., Oswin H. (1957) J. Electrochem. Soc. **9**: 104
[16] Lakhtin Y. (1971) Engineering Physical Metallurgy. Mir publishers, Moscow
[17] Uhlig H. H. (1963) Corrosion and Corrosion Control, 2nd edn. John Wiley, p. 30
[18] Uehara J., Aramaki K. (1991) J. Electrochem. Soc. **138**(11): 345
[19] Khamis E., Bellucci F., Latanision R. M., El-Ashry E.SH. (1991) Corrosion **47**(9): 667
[20] Masfeld E. (1987) Corrosion Mechanisms. Marcel Dekker, p 119
[21] Shams El-Din A. M., Abd El-Haleem S. M. (1973) Werkstoffe Korros. **24**: 389

Received July 19, 1994. Accepted (revised) August 29, 1994